McKenzie, J.A., Davies, P.J., Palmer-Julson, A., et al., 1993
Proceedings of the Ocean Drilling Program, Scientific Results, Vol. 133

13. PRELIMINARY RESULTS OF PALEOTEMPERATURE RECONSTRUCTION USING THE MAGNESIUM TO CALCIUM RATIO OF DEEP-SEA OSTRACODE SHELLS FROM THE LATE QUATERNARY OF SITE 822, LEG 133 (WESTERN CORAL SEA)[1]

Thierry Corrège[2]

ABSTRACT

Analyses of living benthic ostracodes collected in the Coral Sea show a direct relationship between water temperature and the Mg/Ca ratio in the ostracode shells. Fossil ostracodes from Hole 822A (western edge of the Queensland Trough) were analyzed for their Mg and Ca content, and paleotemperatures are inferred using equations derived from the modern material. The bottom-water temperature record from Site 822, spanning the last 120,000 yr, indicates substantial cooling during glacial periods. It also documents important variations during an interval that is considered to correspond to isotopic stage 5. Although still preliminary, these results show that trace-element analyses of ostracode shells have a great potential for paleoceanographic studies.

INTRODUCTION

The main purpose of this study is to apply to late Quaternary microfossils the newly established method of paleotemperature reconstruction using trace-element analysis of benthic ostracode shells (Corrège and De Deckker, unpubl. data).

Site 822, situated in 955 m of water on the western slope of the Queensland Trough, was selected for several reasons. Given the depth of Site 822, there was a high probability that ostracodes required for this research would be encountered in the core samples. It was also anticipated that the change in water temperature registered between glacial and interglacial stages at that depth, compared to deeper sites, would be large enough for detection with the new technique. In addition, the position of Site 822 within the top portion of the Antarctic Intermediate Water makes it a good site for future study of the vertical movements through time of this particular watermass.

MATERIAL AND METHODS

Material

The top 27 m of Hole 822A, corresponding to lithologic Subunit IA, was sampled every 25 cm. The sediment is a clayey bioclastic calcareous ooze that exhibits some change in color (see core description in Davies, McKenzie, Palmer-Julson, et al., 1991). Benthic ostracodes were extracted from each core sample for trace-element analysis. Ostracodes are microscopic crustaceans enclosed in a bivalve shell made of low-magnesium calcite. They are commonly used in paleoenvironmental studies (De Deckker et al., 1988).

Methods

Preparation and Analysis

For each core sample, ~5 cm^3 of sediment was placed in a solution of 3% hydrogen peroxide for at least two weeks to eliminate organic matter and to separate the clays. Each sample was then washed through a 100-µm sieve and dried at 40°C. The ostracodes were extracted using conventional techniques under a binocular microscope, and the following were observed in the faunal assemblages: presence of partial dissolution of the valves, faunal contamination by shallow-water taxa, and size sorting (see explanations below). Adults of the characteristic deep-sea genera *Krithe* and *Bythocypris* were prepared for trace-element analyses. Individual valves were cleaned in an ultrasonic bath for a short period of time (typically 1–2 s to avoid breakage of the valves) and checked under a high-power microscope for any adhering particles. Only visibly cleaned specimens were used for chemical analysis. Ethanol was used as a medium for observation under the microscope and during cleaning procedures, because it has a lower viscosity and dries faster than water. Each individual clean valve was dissolved in 10 mL of high-purity 2% HNO_3 and analyzed for its Ca and Mg content. Analyses were conducted using a GBC 906 atomic absorption (AA) spectrophotometer. Concentrations of Ca were determined by flame analysis (detection limit: 0.02 ppm), using a cesium buffer, whereas concentrations of Mg were determined using both flame and graphite furnace analyses (detection limit on the furnace: 0.01 ppb). For each individual valve analyzed, three replicates were run for the two elements. The values of the standard deviation were always <5% and typically on the order of 2% for Mg. Repetitive runs using standards of different concentrations gave a typical error of 8% for both elements.

Microscope Observations

Supplementary observations of the ostracode fauna were tabulated (Fig. 1) as follows:

1. Dissolution index, with values theoretically ranging from 1 (100% of clear valves in pristine condition of preservation) to 5 (100% of opaque/white valves). Usually, when ostracodes are alive, both valves are transparent. After the death of the animal, partial dissolution can affect the valves, which tend to become an opaque white. None of the 107 samples observed showed perfect preservation (value 1) or advanced dissolution (value 5) of the ostracode shells.
2. Contamination index, with a value of 1 (0%–10% contaminants) or 2 (between 10% and 50% contaminants). None of the samples contained more than 50% contamination by shallow-water ostracodes. In some areas of the Coral Sea, shallow material transported downslope can affect the composition of the sediment, to such an extent that shallow-water ostracodes can account for more than 50% of the total ostracode fauna (Corrège, unpubl. data).
3. Sorting index, with a value of 1 for a normal assemblage (all sizes, ranging from small juvenile valves to larger adult valves) and 2 for a sorted assemblage (Oertli, 1971).

The three indexes were plotted vs. sample depth to assess the reliability of the trace-element analysis (Fig. 1). Sorting and contami-

[1] McKenzie, J.A., Davies, P.J., Palmer-Julson, A., et al., 1993. *Proc. ODP, Sci. Results,* 133: College Station, TX (Ocean Drilling Program).
[2] Department of Geology, Australian National University, Canberra, Australia.

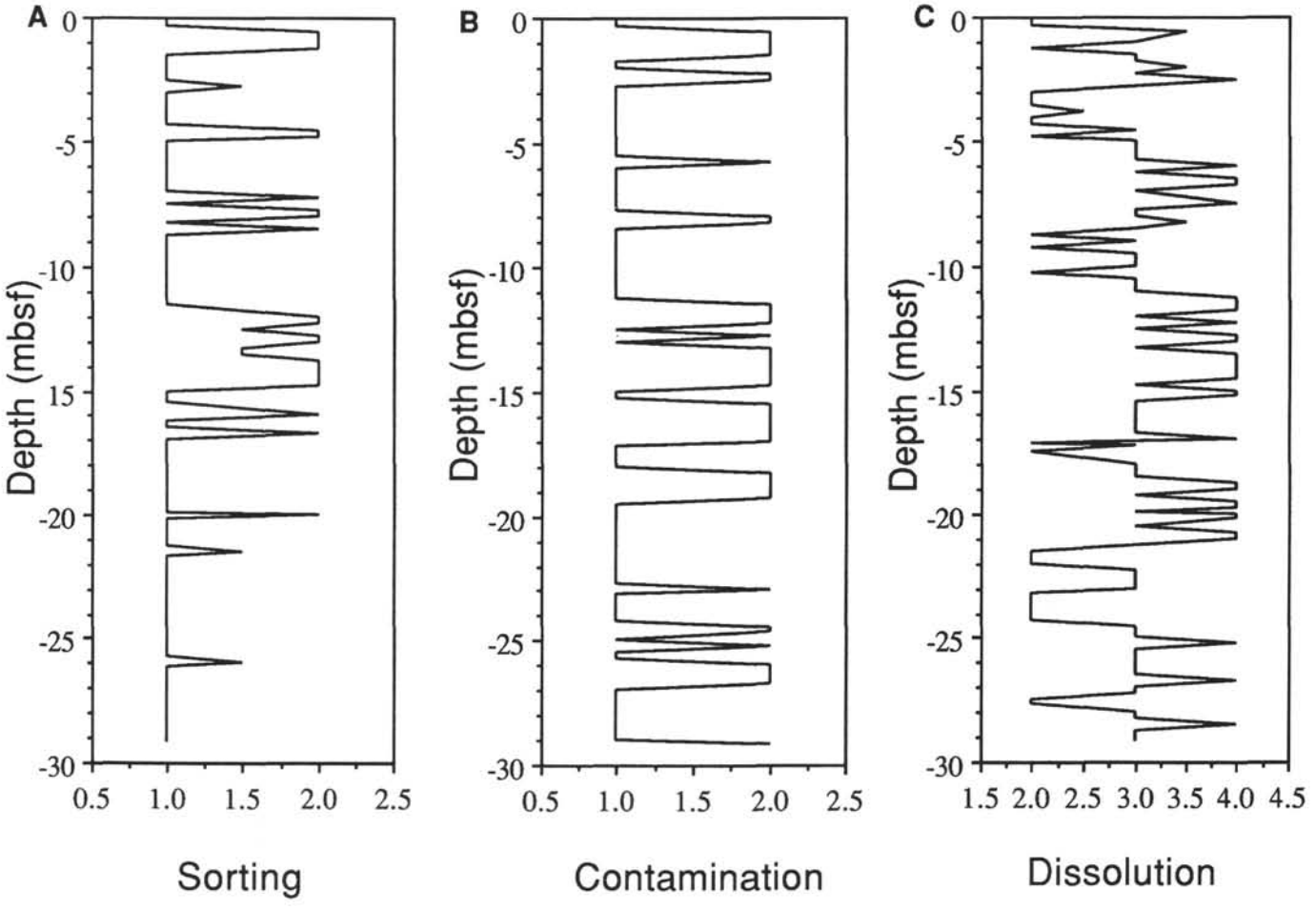

Figure 1. **A.** Plot of sorting index vs. sample depth in the core (see text for explanation). **B.** Plot of contamination index vs. sample depth in the core (see text for explanation). **C.** Plot of dissolution index vs. sample depth in the core (see text for explanation).

nation can explain unusually high paleotemperature values, because these parameters reflect downslope transport (although sorting can result from bottom currents as well). The record of dissolution is used to demonstrate that low Mg/Ca ratios are not caused by partial dissolution of the ostracode valves, which may cause preferential loss of Mg (Chivas et al., 1986).

RESULTS

Calibration

We have established a direct relationship between the Mg content of individual ostracode valves (made of low-Mg calcite) and the temperature of the water in which the animal lives (Corrège and De Deckker, unpubl. data). Earlier attempts to establish such a relationship in the marine environment were somewhat inconclusive (Cadot and Kaesler, 1977; Bodergat, 1983), but work on nonmarine ostracodes yielded positive results (Chivas et al., 1983, 1986). By analyzing modern valves of *Krithe* and *Bythocypris* from grab samples collected from the seafloor at different water depths (and hence different temperatures) in the western Coral Sea, we were able to develop calibration curves to link the Mg/Ca molar ratio of individual ostracode valves with water temperature (Fig. 2). This Mg/Ca ratio in the ostracode valve is also affected to a much lesser extent by the Mg/Ca content of ambient water, but this phenomenon is considered to have had a negligible effect during the late Quaternary because of the long residence time of Mg and Ca in seawater. From calibration curves we obtained using modern material, we derived the following equations:

for *Krithe,*

$$T = -2.56 + 462.96(\mathrm{Mg/Ca})_{\mathrm{valve}},\ R^2 = 0.900 \quad (1)$$

for *Bythocypris,*

$$T = -6.45 + 364.16(\mathrm{Mg/Ca})_{\mathrm{valve}},\ R^2 = 0.942 \quad (2)$$

where T = temperature and all Mg/Ca ratios are molar ratios. These equations were calculated for $(\mathrm{Mg/Ca})_{\mathrm{seawater}} = 5.2$ (standard value of modern seawater).

Different species grouped within the same genus have been shown to have similar partition coefficients (Chivas et al., 1986). Therefore, Equations 1 and 2 are valid for any given species of *Krithe* or *Bythocypris,* respectively. Indeed, several species of *Krithe,* and two species of *Bythocypris* were used in this study.

Each point on these calibration curves represents the mean value for the sample, with the associated standard deviation. I analyzed between 5 and 10 individual valves for each sample from a specific depth. It must be noted that analysis of modern material is currently in progress to refine these calibration curves, and therefore, these results should be considered to be only of a preliminary nature.

The calibration curves (Fig. 2) show that a certain spread in the data is to be expected. Thus, one must analyze at least five individual valves (and ideally 8–10 valves)/sample and then average these Mg/Ca values to get a representative ratio. Unfortunately, ostracodes suitable for trace-element analyses were scarce for the size of samples obtained from Hole 822A, and in most cases, I had to deal with one or two valves of the selected genera/sample. Nevertheless, some samples did yield a sufficient number of valves to permit a temperature reconstruction.

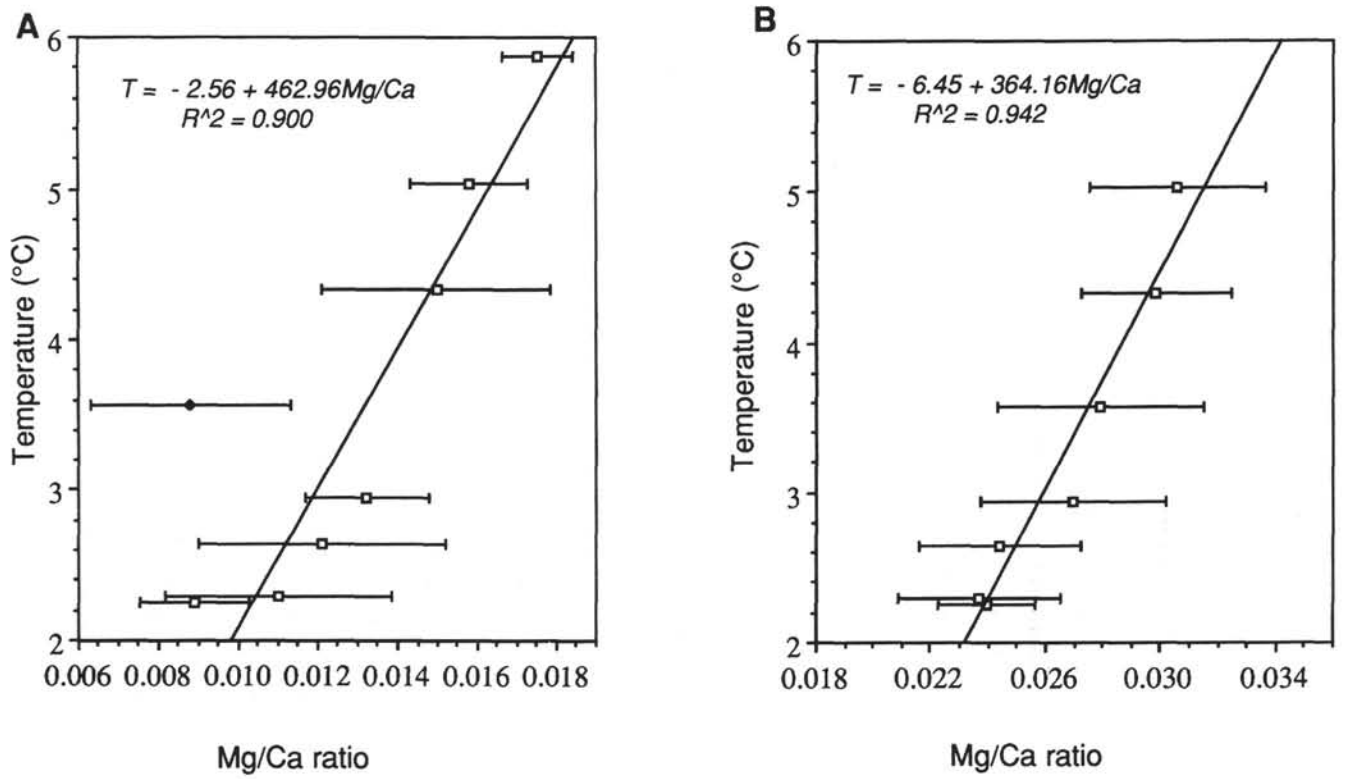

Figure 2. **A.** Calibration curve derived from analyses of Mg/Ca molar ratios in modern *Krithe* from a range of water temperatures. The regression line is based on the mean Mg/Ca value of seven samples (squares). The anomalous sample (diamond) was not included in the calculation of the regression line. Error bars indicate standard deviation of the mean for each sample. **B.** Calibration curve derived from analyses of Mg/Ca molar ratios in modern *Bythocypris* from a range of water temperatures (see **A** for explanations).

Fossil Material

Results from the trace-element analysis of the fossil ostracodes are given in Table 1 and Figure 3. For each individual ostracode analyzed, the Mg/Ca molar ratio is given, together with the paleotemperature value derived from the equation that corresponds to the genus.

Of the 107 samples examined, <60 yielded suitable ostracodes for trace-element analysis. The best set of samples is available in the top 11 m of the hole (Fig. 4). Between 11 and 17 meters below seafloor (mbsf), high numbers of shallow ostracodes can be seen, which is indicative of downslope contamination. Between 17 and 27 mbsf *Krithe* and *Bythocypris* are too scarce to provide reliable temperature reconstructions.

One encouraging result is that in the case of samples containing both *Krithe* and *Bythocypris,* the temperature estimates obtained from the two ostracode genera frequently give similar values.

If only one valve is analyzed, the typical error of the paleotemperature value is of the order of ±1°C. In the case of samples having three or four valves analyzed, this error is lowered to ±0.6°–0.5°C, depending on the standard deviation.

One concern with this paleotemperature reconstruction is the absence of an age control. In the absence of oxygen-isotope data, the only biostratigraphic marker I could use was the pink form of *Globigerinoides ruber,* which disappeared 120,000 yr ago (Thompson et al., 1979). This event is situated between 8.75 and 9.0 mbsf in Hole 822A, giving an average sedimentation rate of 7.5 cm/k.y. for the top 9 m of the core. I used this sedimentation rate to derive an age model for the upper 9 m of Hole 822A. I am well aware of the inaccuracy of this model (variable sedimentation rate, top of the section probably missing because of disturbance during the positioning of the drill). However, in the absence of an alternative way of dating the core, this is all I can rely on.

The first sample containing more than two ostracodes is situated at 1.5 mbsf. It provides a paleotemperature of 4.9°C, but shallow-water ostracodes are present in the sample. This may indicate that the ostracodes analyzed came from upslope, thus, from water warmer than the actual site of Hole 822A. The next reliable sample is situated at 4.25 mbsf, and it gives a paleotemperature of 4.3°C. Between 1.5 and 4.25 mbsf, the general trend points to a cooling of the water. The age at 4.25 mbsf is interpreted to be ~60,000 yr ago, roughly corresponding to the middle of isotopic stage 3. Data indicate another cooling below 4.25 mbsf, then a warming down to 6.25 mbsf. According to my age model, this is where isotopic stage 5a (~80,000 yr ago) is placed. Another cooling took place between 6.25 and 9.0 mbsf, before the temperature returned to ~4.3°C. This is where I document the first appearance of pink *G. ruber* in the core, thus dating this level at 120,000 yr ago.

DISCUSSION

The present-day water temperature at Site 822 (water depth 955 m) lies between 5.5° and 4.5°C (estimated from a large database of bottom-water temperatures and temperature profiles from the western Coral Sea; Corrège, unpubl. data from various sources).

Examination of the paleotemperature curve in Figure 4 shows that most of the values lie below 5°C, which would tend to indicate that the water was cooler during glacial times at Site 822.

Because of the bathymetric position of Site 822, one has to remember that the difference in sea level between glacial and interglacial times should also be taken into account when looking at the paleotemperature results. In the western Pacific Ocean, the last glacial lowstand was situated 130 m below the present sea level (Chappell and Shackleton, 1986). Today in the Coral Sea, the difference in temperature between 955 and 825 m is of the order of 0.7°C (taken from the above-mentioned database). This means that if bottom-water

Table 1. Geochemical analyses of ostracode shells from Site 822.

Depth (mbsf)	Sample code	Mg (meq/L)	Ca (meq/L)	Mg/Ca	Mg/Ca mean	St. dev. Mg/Ca	Temperature (°C)
0.1	K1A	0.000534	0.039743	0.013426	0.013082	0.000345	3.49
0.1	K1B	0.000595	0.046736	0.012737			
1.0	K3A	0.000406	0.027840	0.014569	0.014569		4.18
1.5	B5A	0.001134	0.035840	0.031627	0.031180	0.002290	4.90
1.5	B5B	0.001448	0.042928	0.033734			
1.5	B5C	0.001127	0.040008	0.028178			
1.75	K6A	0.000911	0.066450	0.013716	0.013716		3.79
2.0	K7A	0.001277	0.111958	0.011405	0.011405		2.72
3.75	K10A	0.000608	0.052625	0.011546	0.011546		2.78
4.0	K11B	0.000745	0.059408	0.012538	0.012538		3.24
4.0	B11A	0.001138	0.040282	0.028254	0.027962	0.000292	3.73
4.0	B11B	0.001365	0.049326	0.027670			
4.25	K12A	0.000975	0.058355	0.016702	0.014837	0.002446	4.31
4.25	K12B	0.000813	0.076302	0.010651			
4.25	K12C	0.000645	0.039444	0.016343			
4.25	K12D	0.000325	0.020793	0.015650			
5.0	B13A	0.001712	0.068017	0.025168	0.025168		2.71
5.25	K14A	0.001208	0.095074	0.012701	0.012701		3.32
5.5	K15A	0.000802	0.061734	0.012990	0.012990		3.45
6.25	K16A	0.000827	0.067349	0.012274	0.015123	0.002706	4.44
6.25	K16B	0.000583	0.031074	0.018760			
6.25	K16C	0.000680	0.047444	0.014335			
6.5	K17A	0.000659	0.050958	0.012923	0.013239	0.000316	3.57
6.5	K17B	0.000800	0.059049	0.013555			
6.5	B17A	0.002452	0.088241	0.027788	0.027788		3.66
6.75	B18A	0.001821	0.083280	0.021870	0.022012	0.000142	1.56
6.75	B18B	0.001366	0.061679	0.022153			
7.5	B20A	0.002210	0.100015	0.022096	0.022230	0.000102	1.64
7.5	B20B	0.001710	0.076547	0.022343			
7.5	B20C	0.002830	0.127176	0.022252			
8.0	K21A	0.000836	0.078364	0.010666	0.010666		2.38
8.25	K22A	0.000592	0.055465	0.010677	0.010677		2.38
8.25	B22A	0.002691	0.098996	0.027184	0.026522	0.000662	3.20
8.25	B22B	0.003300	0.127620	0.025860			
8.75	K23A	0.000481	0.029297	0.016424	0.016424		5.04
9.0	K24A	0.000600	0.039040	0.015367	0.014904	0.001071	4.34
9.0	K24B	0.000635	0.043027	0.014767			
9.0	K24C	0.000802	0.060416	0.013274			
9.0	K24D	0.000443	0.027311	0.016207			
9.25	K25A	0.000862	0.068651	0.012557	0.012557		3.25
9.25	B25A	0.002344	0.107686	0.021768	0.021768		1.47
9.5	K26A	0.000620	0.052410	0.011829	0.011601	0.000228	2.81
9.5	K26B	0.000635	0.055869	0.011373			
9.75	K27B	0.000620	0.039379	0.015743	0.015743		4.73
9.75	B27A	0.002872	0.094305	0.030450	0.030450		4.63
10.5	B29A	0.002216	0.076193	0.029086	0.029086		4.14
11.25	K31A	0.000861	0.065926	0.013053	0.013321	0.000268	3.60
11.25	K31B	0.001147	0.084438	0.013589			
17.14	K41A	0.000478	0.034707	0.013775	0.013775		3.81
17.5	K42A	0.000358	0.024720	0.014473	0.014473		4.14
18.25	K44A	0.000648	0.049047	0.013206	0.012342	0.000865	3.15
18.25	K44B	0.000527	0.045957	0.011477			
18.75	K45A	0.000424	0.028663	0.014796	0.014796		4.29
19.9	K46A	0.002745	0.091375	0.030042	0.030042		4.49
21.0	B47A	0.003455	0.143426	0.024086	0.024086		2.32
22.5	K48B	0.000962	0.063835	0.015075			4.42
23.5	K49A	0.000575	0.040896	0.014066	0.016134	0.002068	4.91
23.5	K50B	0.000831	0.045668	0.018202			
24.0	B51A	0.001038	0.039683	0.026154	0.026154		3.07
27.0	K59A	0.000601	0.054117	0.011114	0.011114		2.58

When more than one valve was analyzed in a sample, the mean Mg/Ca and the associated standard deviation were calculated. For these samples, the paleotemperature was calculated from the mean Mg/Ca.

temperature at Site 822 had not changed between the last glacial and today, paleotemperature values for the last glacial should be around 5.2° to 6.2°C. My data demonstrate that this is clearly not the case, thus implying a cooling of the Coral Sea's intermediate waters.

Paleotemperature reconstructions from oxygen isotopic composition of benthic foraminifers show that the deep Pacific Ocean was between 1.5° and 1.1°C cooler during the last glaciation (Chappell and Shackleton, 1986; Birchfield, 1987). My data indicate that the intermediate waters in the Coral Sea were also cooler during the last glacial episode, with a temperature gradient possibly higher than 2°C.

The deadline for submitting this chapter forced me to use equations for paleotemperatures that are still at a preliminary stage. I am still in the process of analyzing modern samples that might slightly alter the present calibration curves used here. In particular, I expect that the slope of the calibration curves might be lower. This would tend to reduce the absolute difference between high Mg/Ca ratios (indicative of high temperatures) and low Mg/Ca ratios (indicative of low temperatures). One consequence would be to increase the values of temperature corresponding to low Mg/Ca ratios. At the moment, the paleotemperature values at 6.75 and 7.50 mbsf seem too low. To

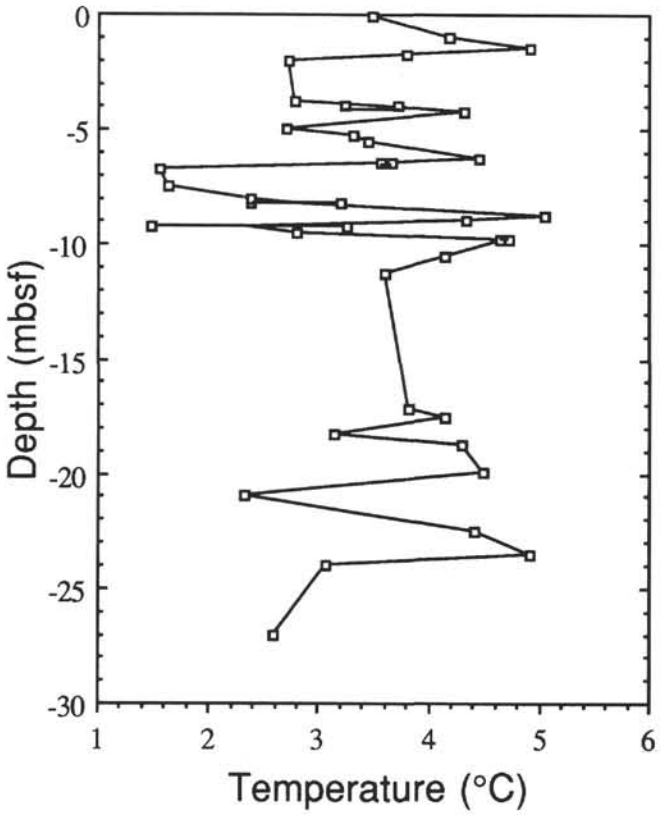

Figure 3. Paleotemperature curve for the upper 27 m of Hole 822A (see Table 1 for detail of values used to calculate each point).

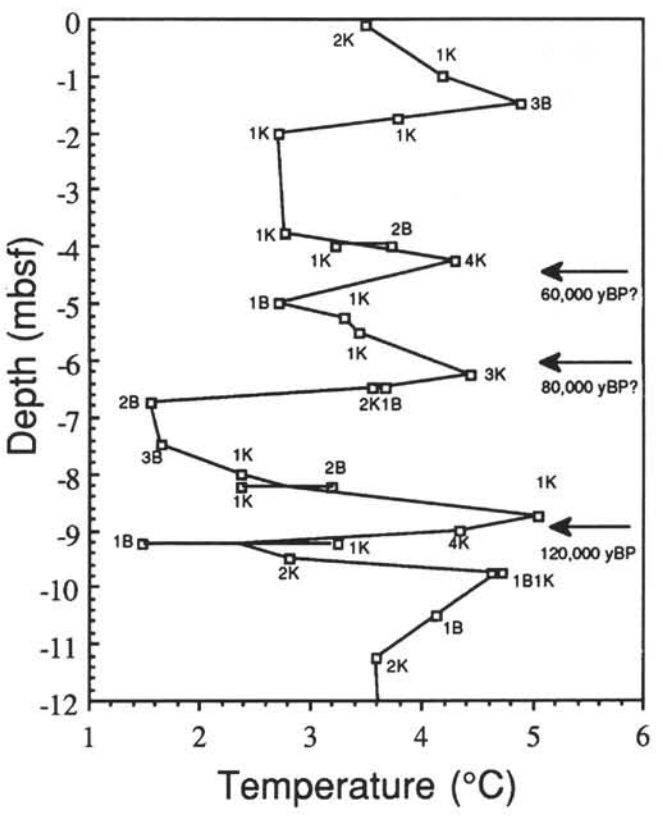

Figure 4. Reconstructed paleotemperature curve for the upper 12 m of Hole 822A. The 120,000-yr-B.P. datum is based on the disappearance of the pink form of *Globigerinoides ruber,* and the other ages are extrapolated assuming a constant sedimentation rate. The number of valves and the genus analyzed are shown on each point of the curve (K = *Krithe* and B = *Bythocypris*). See Table 1 for detail of values used to calculate each point.

obtain water temperatures lower than 2°C at a depth less than 1000 m in the Coral Sea appears improbable since such temperatures are found today only below 4000 m. The only possible explanation could be the formation of coastal upwellings during glacial times, but there is no other evidence to support this hypothesis.

One intriguing result from my reconstruction is the important decrease in water temperature situated between the two "highs" at 9 and 6.5 mbsf (corresponding respectively to isotopic stages 5e and 5a, according to my age model). If correct, my data indicate that oceanographic variations within isotopic stage 5 were probably more marked in the tropical Pacific Ocean than originally thought (e.g., Shackleton, 1987).

Because low Mg/Ca ratios (and, hence, low temperatures) occur mostly during times of high dissolution, one might think that the low ratios are in fact the result of partial dissolution of the ostracode shells, with a loss of Mg. This is unlikely for several reasons. First, I tried to use only ostracodes that did not exhibit any sign of dissolution. Second, experience with freshwater and brackish ostracodes showed that Mg is lost quickly once dissolution of the shells occurs (De Deckker, pers. comm., 1992). Moreover, the correlation between low Mg/Ca ratio and high dissolution is not always true, and one can get low Mg/Ca ratios for samples that do not exhibit any sign of dissolution.

CONCLUSIONS

Although this work is still in progress, I postulate that the Mg/Ca ratio of ostracode shells has great potential for reconstructing past bottom-water temperatures in the world oceans. This is the first geochemical method that depends only on temperature (at least for the late Quaternary, when $[Mg/Ca]_{seawater}$ remained unchanged), as opposed to oxygen isotope ratios. In fact, a coupling of the two methods should permit better assessment of the relative importance of temperature and ice volume changes in the $\delta^{18}O$ signal (Chivas et al., in press).

The main result from my investigation has been the documentation of a substantial change in temperature in the Queensland Trough during the last 120,000 yr. The amplitude of these variations is still difficult to estimate because of the few data available for Hole 822A, and also because the calibration curves still require additional data.

The next step of my research will involve analysis of ostracodes from deeper cores to document the temperature gradient difference in the Coral Sea between the present and the last glacial episode.

ACKNOWLEDGMENTS

Many thanks to Patrick De Deckker (ANU) for useful discussions and for correcting early versions of this manuscript. I also thank Peter Davies (University of Sydney), David Steel (ANU) for help with the AA, Dereck Burrage (AIMS), the captain and crew of the *Franklin* for help during collection of modern ostracodes, and Brian Funnell and Anne Marie Bodergat for their constructive review of this manuscript. This research is supported by an ANU Ph.D. scholarship.

REFERENCES*

Birchfield, G.E., 1987. Changes in deep-water $\delta^{18}O$ and temperature from the last glacial maximum to present. Paleoceanography, 2(4):431–442.

* Abbreviations for names of organizations and publications in ODP reference lists follow the style given in *Chemical Abstracts Service Source Index* (published by American Chemical Society).

Bodergat, A.M., 1983. Les ostracodes, témoins de leur environnement: approche chimique et écologique en milieu lagunaire et océanique. *Docum. Lab. Géol. Lyon,* 88:1–246.

Cadot, H.M., and Kaesler, R.L., 1977. Magnesium content of calcite in carapaces of benthic marine Ostracoda. *Paleont. Contr. Univ. Kansas,* 87:1–23.

Chappell, J., and Shackleton, N.J., 1986. Oxygen isotopes and sea level. *Nature,* 324:137–140.

Chivas, A.R., De Deckker, P., Shelley, J.M.G., 1983. Magnesium, strontium and barium partitioning in nonmarine ostracode shells and their use in paleoenvironmental reconstructions. A preliminary study. *In Maddocks, R.F. (Ed.), Applications of Ostracoda*: Houston (Uni. Houston Geosci.), 238-249.

————, 1986. Magnesium and strontium in nonmarine ostracod shells as indicators of palaeosalinity and palaeotemperature. *Hydrobiologia,* 143:135–142.

Chivas, A.R., De Deckker, P., Cali, J.A., Chapman, A., Kiss, E., and Shelley, J.M.G., in press. Coupled stable-isotope and trace-element measurements of lacustrine carbonates as paleoclimatic indicators. *Proc. Chapman Conf. on Continental Isotopic Indicators of Climate.* Am. Geophys. Union.

Davies, P.J., McKenzie, J.A., Palmer-Julson, A., et al., 1991. *Proc. ODP, Init. Repts., 133: College Station (Ocean Drilling Program).*

De Deckker, P., Colin, J.P., Peypouquet, J.P., 1988. Ostracoda in the earth sciences: Amsterdam (Elsevier).

Oertli, H.J., 1971. The aspect of ostracode faunas. A possible new tool in petroleum sedimentology. *Bull. Centre Recherche SNPA Suppl.,* 5:137–151.

Shackleton, N.J., 1987. Oxygen isotopes, ice volume and sea level. *Quat. Sci. Rev.,* 6:183–190.

Thompson, P.R., Duplessy, J.C., and Bé, A.H., 1979. Disappearance of pink-pigmented *Globigerinoides ruber* at 120,000 yr B.P. in the Indian and Pacific oceans. *Nature,* 280:554–558.

Date of initial receipt: 1 June 1992
Date of acceptance: 14 January 1993
Ms 133B-222